Journal of Biomolecular NMR (2006) 34: 237–244
DOI 10.1007/s10858-006-0024-8

Article

Combining NMR relaxation with chemical shift perturbation data to drive protein–protein docking

Aalt D.J. van Dijk, Robert Kaptein, Rolf Boelens & Alexandre M.J.J. Bonvin*
NMR Research Group, Bijvoet Center for Biomolecular Research, Utrecht University, 3584CH, Utrecht, The Netherlands

Received 25 November 2005; Accepted 31 January 2006

Key words: computational docking, NMR relaxation, protein complex, structure calculation

Abstract

The modeling of biomolecular complexes by computational docking using the known structures of their constituents is developing rapidly to become a powerful tool in structural biology. It is especially useful in combination with even limited experimental information describing the interface. Here we demonstrate for the first time the use of diffusion anisotropy in combination with chemical shift perturbation data to drive protein–protein docking. For validation purposes we make use of simulated diffusion anisotropy data. Inclusion of this information, which can be derived from NMR relaxation rates and reports on the orientation of the components of a complex with respect to the rotational diffusion tensor, substantially improves the docking results.

Introduction

A major innovation in modeling biomolecular complexes/interactions has been the development of docking algorithms that aim to elucidate the structure of a complex based on the known structures of its constituents (Halperin et al., 2002; van Dijk et al., 2005b). The docking process can be facilitated by inclusion of experimental information such as the NMR chemical shift perturbations (CSP) that are observed when titrating the molecules together (Clore and Schwieters, 2003; Dominguez et al., 2003; van Dijk et al., 2005b). The structure determination of biomolecules by NMR, which is traditionally based mainly on NOEs, has progressed recently by including new experimental information, most notably residual dipolar couplings (RDCs) (Fushman et al., 2004; Bax and Grishaev, 2005) and diffusion anisotropy (relaxation) data (Fushman et al., 2004) which contain valuable long-range orientational information. It has previously been shown that the inclusion of RDCs into docking improves the results (Clore and Schwieters, 2003; Dobrodumov and Gronenborn, 2003; van Dijk et al., 2005a).

Diffusion anisotropy data have been used previously in various ways to characterize biomolecular complexes. One approach is to fit the data to the structures of the individual components and align the resulting tensors (Bruschweiler et al., 1995; Hwang et al., 2001; Fushman et al., 2004). It is also possible to compare back-calculated and experimental relaxation data to select various structural models (Barbato et al., 1992; Fushman et al., 1999; Bernado et al., 2003). Relaxation data have also been used as restraints in NMR structure calculations to refine a multi domain protein structure in combination with classical NOE information (Tjandra et al., 1997; Hashimoto et al., 2000). Here we demonstrate that NMR relaxation data can be used to drive

*To whom correspondence should be addressed. E-mail: a.m.j.j.bonvin@chem.uu.nl

protein–protein docking in combination with chemical shift perturbation data. These data have been implemented as additional restraints in our data-driven docking approach HADDOCK (Dominguez et al., 2003) that encodes experimental information about interaction surfaces into ambiguous interaction restraints (AIRs). Compared to the use of RDCs, relaxation data do not require dissolving the protein complexes in liquid crystalline media and can be measured from regular solution samples, which can offer a serious advantage.

Methods

Structures and data

Docking was performed on the E2A–HPr complex (PDB 1GGR) (Wang et al., 2000), using the structures of the unbound components, 1F3G (Worthylake et al., 1991) and 1HDN (van Nuland et al., 1994), respectively. Histidine 90 on E2A was used in its phosphorylated form. Experimental chemical shift perturbation data (Chen et al., 1993) were introduced in the form of AIRs as described previously (Dominguez et al., 2003). In all docking runs, 50% of the AIRs were randomly removed, a procedure which helps to deal with inaccuracies and false positives in the chemical shift perturbation data.

Theoretical relaxation data were generated with HydroNMR (de la Torre et al., 2000), using a shell thickness parameter of 2.4 Å (this represents the sum of the average atomic van der Waals radius plus the thickness of the hydration shell). HydroNMR uses the "shell-modeling" strategy where a shell-model composed of 'mini-beads' of radius σ is derived from the primary hydrodynamic model, and extrapolation to the limit $\sigma = 0$ is carried out. We used the option NSIG = −1, which means that the program estimates the extrapolation limits. The hydrodynamic calculations were performed using a temperature $T = 300$ K, a viscosity $\eta = 7\times 10^{-4}$ kg/(m s) and a field strength of 600 MHz. The output of HydroNMR consists of T_1 and T_2 relaxation times and heteronuclear NOE as well as the rotational diffusion tensor. The latter was used to generate three additional artificial sets of relaxation data in CNS (Brunger et al., 1998): the tensor orientation was kept but larger anisotropy and/or rhombicity were defined, in order to probe the influence of these parameters on the docking results. Note that three parameters are needed to describe the magnitude of the rotational diffusion tensor components. These can be either τ_c, Da and R, or Dx, Dy and Dz, which are related to another via: $\tau_c = 0.5/(Dx + Dy + Dz)$, $Da = 2Dz/(Dx + Dy)$ and $R = 1.5(Dy - Dx)/(Dz - 0.5(Dx + Dy))$. In our case, τ_c was 9.8 ns for all sets; the original parameters calculated by HydroNMR (set1) are $Da = 1.35$ and $R = 0.33$; for the other three sets these are 1.35 and 0.7 (set2), 1.8 and 0.33 (set3) and 1.8 and 0.7 (set4), respectively. Dx, Dy and Dz for set1 are given by 1.5, 1.6 and 2.1×10^7 s^{-1}, for set2 by 1.4, 1.7 and 2.1×10^7 s^{-1}, for set3 by 1.2, 1.5 and 2.4×10^7 s^{-1}, and for set4 by 1.1, 1.6 and 2.4×10^7 s^{-1}, respectively.

In order to investigate the influence of experimental noise we generated additional data sets by adding 2% or 5% noise on both T_1 and T_2 for each set defined above. Note that 2% corresponds to a typical experimental noise level while 5% is already pretty high. We used only data from secondary structure elements (70 out of 150 residues for E2a and 57 out of 85 for HPr) for the docking. This somewhat mimics the filtering that is often performed to exclude residues affected by flexibility and/or chemical exchange. (Note that our theoretical data do not suffer from such effects.)

Relaxation data as restraints in docking

The use of relaxation data as restraints in NMR structure calculations is described in (Tjandra et al., 1997). These have been implemented in various software, among which XPLOR-NIH (Schwieters et al., 2003), SCULPTOR (Hus et al., 1999), and CNS (Brunger et al., 1998). In the latter, the relaxation data are introduced into an energy function defined as:

$$E_{\mathrm{dani}} = k_{\mathrm{dani}}\left(\left(\frac{T_1}{T_2}\right)_{\mathrm{exp}} - \left(\frac{T_1}{T_2}\right)_{\mathrm{back}}\right)^2. \qquad (1)$$

Here $(T_1/T_2)_{\mathrm{exp}}$ is the ratio of experimental relaxation times and $(T_1/T_2)_{\mathrm{back}}$ the back-calculated ratio. For the latter, a floating diffusion tensor is used during the structure calculations. We used a 'square potential' with an error range of 0.2;

if the difference between experimental and back-calculated values is lower than this value, E_{dani} is set to 0.

In order to back-calculate T_1 and T_2, the diffusion tensor parameters need first to be determined. In the case of docking, the 3D structures of the isolated components are usually known and can be used to fit the T_1/T_2 ratios. This was done using the software Tensor2 (Dosset et al., 2000). The synthetic relaxation data were fit to the unbound E2A structure and the 10 models of the unbound HPr structure, respectively; the resulting tensor parameters from the best-fitting structure were used subsequently. To probe the influence of the goodness of fit on the tensor parameters, we also did for each of the four sets a docking run using the parameters resulting from the worst fit.

The HADDOCK docking protocol consists of three consecutive stages (for details, see (Dominguez et al., 2003):

(i) randomization of orientations followed by rigid body energy minimization (EM);
(ii) semi-flexible simulated annealing in torsion angle space (TAD-SA), which consists of (ii-a) a rigid body Molecular Dynamics search and first simulated annealing, (ii-b) a second semi-flexible simulated annealing during which side chains at the interface are free to move, and (ii-c) a third semi-flexible simulated annealing during which both side chains and backbone at the interface are free to move; and
(iii) final refinement in Cartesian space with explicit solvent.

Table 1. Force constants used during the different stages of the docking protocol

Stage[a]		k_{dani} (kcal mol^{-1})	k_{air} (kcal mol^{-1} A^{-2})
(i)	Rigid body EM	1–10	1–10
(ii-a)	SA	1–5	10
(ii-b)	SA	5–10	10–50
(ii-c)	SA	10	50
(iii)	Water refinement	10	50

[a]i, ii and iii refer to the rigid body, simulated annealing (SA) and water refinement stages of the protocol, respectively; ii-a, ii-b and ii-c refer to the different parts of the semi-flexible simulated annealing (see Methods for details); k_{dani}, force constant for DANI restraints; k_{air}, force constant for Ambiguous Interaction Restraints.

The tensor is introduced at stage (i) with a random orientation; a rotational minimization is used to find its optimal orientation (this is repeated a few times to find the global minimum). During stages (ii) and (iii) the tensor is free to rotate. The values of the force constants during the various stages of the protocol are listed in Table 1.

After each of the different stages, a score is calculated by using weights for the different energy terms (see Table 2). The rigid body docking stage is performed a number of times (in our case: 5 times), and the best resulting structure of those is saved. Note that after rigid body docking out of 1000 structures, the best 200 based on this score are selected for further refinement.

Results and discussion

Orientational information to distinguish docking solutions

As CSP data do not define the specific contacts that are made across the interface and thus the relative orientation of the components of a complex, distinguishing between different, possibly symmetry-related, binding modes can be difficult. This is indeed a common problem in our data-driven docking approach: symmetry related solutions are obtained where one molecule is rotated by approximately 180° around an axis orthogonal to the binding surface. In favorable cases this ambiguity can be removed by mutagenesis and biochemical methods for screening interactions.

Table 2. Scoring scheme[a] in HADDOCK 2.0_devel

Docking stage term	Rigid body EM	SA	Water refinement
Elec	1.0	0.2	0.2
vdW	0.01	1.0	1.0
BSA	−0.01	−0.01	0.0
Desolv[b]	1.0	1.0	1.0
AIR	0.01	0.1	0.1
DANI	0.01	0.1	0.1

[a]The overall score is calculated as a weighted sum of different terms, using the weights as listed. Elec, electrostatic energy; vdW, van der Waals energy; BSA, buried surface area; Desolv, desolvation energy; AIR, ambiguous interaction restraints; DANI, diffusion anisotropy restraint energy.[b]The desolvation energy is calculated using the atomic desolvation parameters of Fernandez-Recio et al. (2004).

An alternative approach that requires no further biochemical manipulation is the inclusion of anisotropic information. Next to RDCs, relaxation data can also be useful for this purpose (Fushman et al., 2004). To illustrate this, we used Hydro-NMR (de la Torre et al., 2000) to generate a theoretical set of ^{15}N relaxation data (set1) for the E2A–HPr complex (Wang et al., 2000), which were subsequently converted into diffusion anisotropy restraints (Tjandra et al., 1997) in CNS (Tjandra et al., 1997; Brunger et al., 1998). To monitor the ability of this type of information to distinguish between various relative orientations in a complex, one of the two components of the complex was rotated around either the *z*-axis of the diffusion tensor or the *z*-axis of the inertia tensor, both being approximately orthogonal to the interface. This rotation is meant to represent different docking solutions that could be obtained when only information about the interface would be used: since experimental data such as CSP data define in principle the binding interface, there is basically only one rotational degree of freedom left to describe the relative orientation of the two components of the complex. The restraint energy as a function of rotation angle is shown in Figure 1. When the rotation is performed exactly around the diffusion tensor *z*-axis, one finds multiple degenerate minima (one at 0° and one at 180°): this is a well-known characteristic of relaxation data. However, even a small difference between rotation and tensor axes is enough to lift this degeneracy: this is illustrated by the continuous lines in Figure 1 that were obtained by rotating the structures around the *z*-axis of the inertia tensor instead of the diffusion tensor. This second axis would represent the axis of rotation between possible symmetry related docking solutions and its exact orientation will depend on the properties of the binding surface. It has no physical meaning and is not *per se* related to the diffusion tensor axes.

The orientation of the two axes differs by only 5° in this particular case. Explicit modeling of the interaction by computational docking should thus be able to lift the degeneracy present in the relaxation data provided the interface shows some degree of asymmetry, for example, in the chemical shift perturbation data, the electrostatic potential or the surface shape.

When using the unbound structures (which differ slightly from the bound forms), there is an

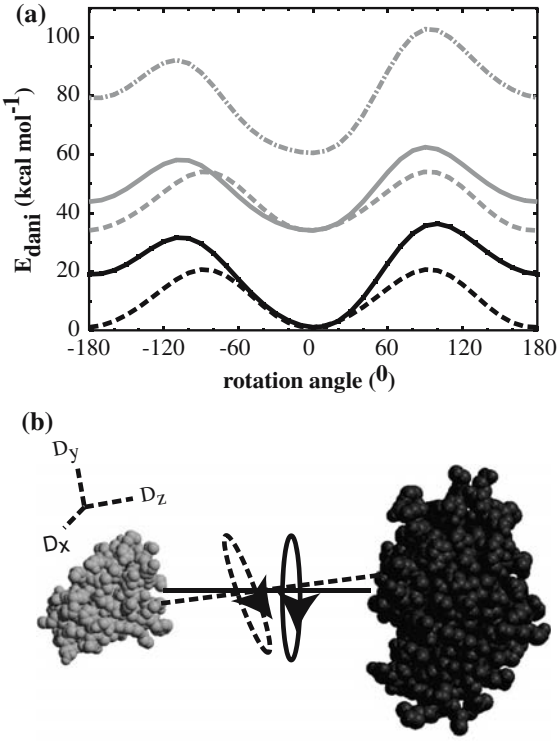

Figure 1. (a) Diffusion anisotropy restraint energy as a function of the rotation angle around the diffusion tensor *z*-axis (dashed lines) or inertia tensor *z*-axis (continuous lines) for the bound (black) and unbound (gray) structures of the E2A–HPr complex. In addition, in the case of the unbound structures, a wrong tensor parameter (Da = 1.5 instead of 1.35) was used on purpose for the rotation around the inertia tensor axis (dash-dotted gray line): this did not affect the position of the minimum. (b) Representation of the rotation around the *z*-axis of the diffusion anisotropy (dashed line) and inertia (continuous line) tensor of the E2A–HPr complex (E2A: black, HPr: gray).

overall upward shift of the curves (gray lines); however, the minimum is still at 0°. For the unbound structures we also tested the effect of wrong Da and *R* values on the shape of the curve. Roughly, errors of up to 20% and 30% in the estimation of Da and *R*, respectively, still result in a minimum at the correct rotation angle, while distorting the curve (this is illustrated in Figure 1 for the case of using an anisotropy of 1.5 instead of the correct value of 1.35).

Relaxation data in docking

The use of relaxation data was implemented in our data-driven docking approach HADDOCK (Dominguez et al., 2003). HADDOCK encodes experimental information about interaction sur-

faces into AIRs. These are defined between any residue which, based on experimental data (e.g., CSP), is believed to be at the interface, and all such residues plus their surface neighbors on the partner molecule. The AIRs are incorporated as an additional energy term into the energy function that one tries to minimize during sampling.

We introduced the relaxation data as additional restraints; the protocol is comparable to the one presented before for RDCs (van Dijk et al., 2005a). Briefly, during the rigid body energy minimization step, the diffusion tensor is introduced with a random orientation. Then, a rotational minimization is used to find its optimal orientation. During the remaining of the protocol, the tensor is free to rotate; for details see Methods. The E2A–HPr complex was docked without and with inclusion of theoretical relaxation data. The latter were obtained with HydroNMR (set1), which predicted an anisotropy Da of 1.35 and rhombicity R of 0.33, and also with CNS using the tensor orientation obtained with HydroNMR but, for testing purposes, a higher anisotropy and/or rhombicity (see Methods; set2: Da = 1.35, $R = 0.7$; set3: Da = 1.8 and $R = 0.33$; set4: Da = 1.8 and $R = 0.7$). These sets were used to probe the influence of the amount of anisotropy on the docking results. AIRs were defined based on the available experimental CSP-data for the complex (Chen et al., 1993). Starting from the unbound conformations, 1000 structures were generated in the rigid body docking phase, out of which 200 were further refined (using semi-flexible simulated annealing and water refinement). The tensor parameters needed as input for the protocol were obtained from the known structures of the unbound constituents using Tensor2 (Dosset et al., 2000) as commonly done for RDCs (see Methods). The best fit was obtained in all cases for E2A; for HPr, similar tensor parameters were obtained, but with somewhat higher χ^2 values. The tensor parameters used in docking are listed in Table 3. Note that the difference in goodness of fit is due to the fact that the unbound E2A structure is closer to its bound form than the HPr structure (which is reflected in the backbone RMSD values between free and bound structures: 0.3 Å for E2A vs. 1.3 (+/−0.1) Å for HPr).

Inclusion of relaxation data in general improves the docking results, even in the case of substantial amounts of noise (Table 4). The HADDOCK score of the resulting structures is plotted against the interface RMSDs from the target in Figure 2 for each of the four 2% noise sets corresponding to various amounts of anisotropy. The interface RMSD is defined as the backbone RMSD from the structure of the complex for those residues making contacts across the interface within a 10.0 Å cutoff. The inclusion of relaxation data results clearly in a larger number of structures with low interface RMSD (see also Table 4) and a larger energy difference between correct and incorrect solutions, which improves the scoring of the solutions. In all cases the scoring of the solutions is improved when diffusion anisotropy data are included, as can be seen from the number of low-RMSD structures among the 10 best-scoring structures (Table 4). For the set with 5% noise, this is still the case, although the

Table 3. Theoretical and fitted tensor parameters for the E2A–HPr complex[a]

	Set1[a]	Set2[a]	Set3[a]	Set4[a]
Theoretical				
τ_c (ns)	9.80	9.80	9.80	9.80
Da	1.35	1.35	1.80	1.80
R	0.33	0.70	0.33	0.70
Best fit for 0% noise set				
τ_c (ns)	9.81	9.77	9.76	9.76
Da	1.26	1.25	1.55	1.52
R	0.44	0.96	0.46	1.00
χ^2/df	0.17	0.18	0.62	0.63
Worst fit for 0% noise set				
τ_c (ns)	9.95	9.91	10.0	10.0
Da	1.24	1.24	1.49	1.52
R	0.51	0.87	0.54	0.94
χ^2/df	0.88	0.92	3.26	3.74
2% noise set				
τ_c (ns)	9.80	9.75	9.77	9.79
Da	1.28	1.23	1.56	1.58
R	0.21	1.11	0.46	0.90
χ^2/df	0.45	0.66	0.88	1.19
5% noise set				
τ_c (ns)	9.83	9.70	9.59	9.58
Da	1.40	1.35	1.40	1.43
R	0.33	1.09	0.70	1.25
χ^2/df	2.79	1.88	3.31	3.26

[a]Set1 is the original set calculated by HydroNMR; set2, set3 and set4 are sets with artificially increased anisotropy and/or rhombicity (see Methods).

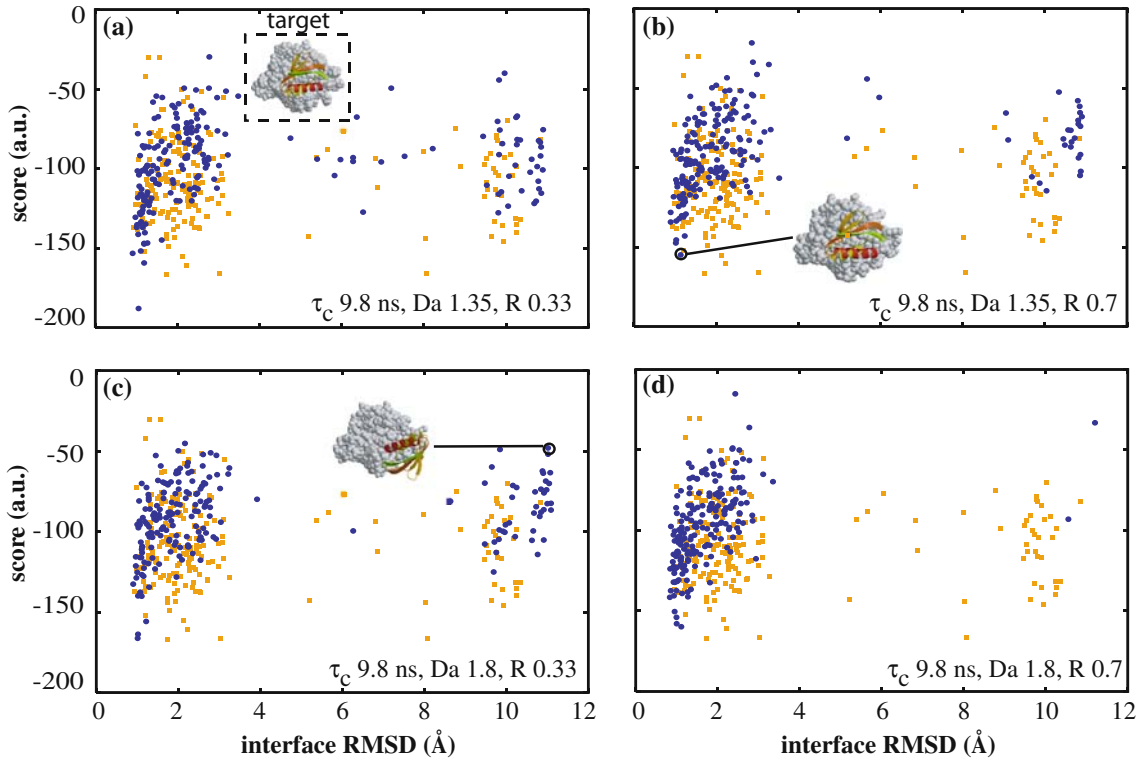

Figure 2. HADDOCK score versus interface RMSDs from the target for docking runs without (orange) and with (blue) relaxation data for various amounts of anisotropy (a) set1; (b) set2; (c) set3; and (d) set4 (see Tables 3 and 4). The reference structure is shown in panel a and examples of docked structures in panels b and c. The HADDOCK score corresponds to the weighted sum of the van der Waals, electrostatic, and restraint energy (DANI + AIR) (see Table 2). The interface RMSDs are calculated on the backbone atoms of the residues making contacts across the interface within a 10.0 Å distance cutoff.

total number (out of 200) of correct solutions varies between the various sets (due to the influence of the tensor parameters). It is also clear from the results in Table 4 that larger anisotropies result in a larger number of correct solutions.

Interestingly, the results from the docking where the worst fit tensor parameters were used are in general still better than the reference docking run without relaxation data. This indicates that the method is not too sensitive to incorrect tensor parameters which is in line with our analysis of the energy function discussed above (see Figure 1).

In the case of docking with relaxation data, structures with large RMSDs have in most cases a low relaxation restraint energy, as they correspond to 180° symmetrical solutions around the tensor axis (see inset in Figure 2c); their interface is however different, resulting in higher AIR and especially electrostatic energies. This is related to the fact that asymmetry in the interface and possibly in the available information describing it (e.g., CSP) is able to lift the degeneracy present in the relaxation data (see above).

One practical limitation of using relaxation data is that chemical exchange and/or flexibility can influence the experimental data. Such effects are absent from our theoretical data sets; however, results obtained in the presence of noise indicate that diffusion anisotropy data will be useful in defining the intermolecular orientation of the components of a complex provided the experimental errors are not too large.

Conformational differences between unbound and bound forms could possibly affect the tensor parameters determined by fitting the data to the unbound components, and thus the docking results. It has however been shown that the tensor parameters can be quite accurately determined even in the presence of substantial experimental errors (Fushman et al., 2004). In addition, our

Table 4. Docking results for the E2A–HPr complex[a]

Docking run	Number of structures with iRMSD[b] < 1/4 Å			
	Rigid body		Refined	
	All 1000	Top 200	All 200	Top 10
Reference	3/376	1/159	3/159	0/7
DANI set1				
No noise	4/414	4/168	3/168	3/10
Worst fit[c]	0/309	0/154	5/155	2/10
2% noise	5/327	5/154	2/154	1/10
5% noise	1/401	1/161	2/161	0/10
DANI set2				
No noise	2/528	1/191	9/191	3/10
Worst fit[c]	3/474	3/191	12/191	4/10
2% noise	2/532	1/190	7/190	4/10
5% noise	4/474	2/196	3/196	2/10
DANI set3				
No noise	4/487	3/192	5/192	0/10
Worst fit[c]	13/441	13/192	26/192	5/10
2% noise	1/481	1/179	11/178	3/10
5% noise	1/511	1/193	5/192	1/10
DANI set4				
No noise	7/544	4/194	20/194	3/10
Worst fit[c]	8/545	7/197	27/197	5/10
2% noise	7/551	5/198	22/198	6/10
5% noise	2/494	2/186	10/185	5/10

[a]One reference docking run was performed using only CSP and no diffusion anisotropy data; docking runs with T_1/T_2 restraints corresponding to various amounts of anisotropy were performed; see Table 3 for the tensor parameters corresponding to the various sets.[b]Interface backbone RMSD from the NMR structure (PDB id 1GGR).[c]Worst fit: docking run using tensor parameters with highest as opposed to lowest χ^2 values (see Table 3).

results obtained with wrong parameters show that the diffusion anisotropy energy (DANI) function is not too sensitive to such errors and still allows to identify the correct minimum as can be seen for the unbound case in Figure 1 (gray dash-dotted curve). This is also illustrated by our docking results using the "worst fit" tensor parameters.

In conclusion, we demonstrated the usefulness of introducing NMR relaxation data in protein–protein docking. These improve the convergence of our docking protocol and both the accuracy and discrimination of the correct solutions. Compared to the use of RDCs, relaxation data have the advantage that their measurement does not require dissolving the protein complexes in liquid crystalline media. This methodology should be useful for the modeling of large protein–protein complexes.

Acknowledgements

This work was supported by a "Jonge Chemici" grant from the Netherlands Organization for Scientific Research (N.W.O.) to A.B.

References

Barbato, G., Ikura, M., Kay, L.E., Pastor, R.W. and Bax, A. (1992) *Biochemistry*, **31**, 5269–5278.

Bax, A. and Grishaev, A. (2005) *Curr. Opin. Struct. Biol.*, **15**, 563–570.

Bernado, P., Akerud, T., de la Torre, J.G., Akke, M. and Pons, M. (2003) *J. Am. Chem. Soc.*, **125**, 916–923.

Brunger, A.T., Adams, P.D., Clore, G.M., DeLano, W.L., Gros, P., Grosse_Kunstleve, R.W., Jiang, J.S., Kuszewski, J., Nilges, M., Pannu, N.S., Read, R.J., Rice, L.M., Simonson, T. and Warren, G.L. (1998) *Acta Crystallogr. D Biol. Crystallogr.*, **54**(Pt 5), 905–921.

Bruschweiler, R., Liao, X.B. and Wright, P.E. (1995) *Science*, **268**, 886–889.

Chen, Y., Reizer, J., Saier, M.H. Jr., Fairbrother, W.J. and Wright, P.E. (1993) *Biochemistry*, **32**, 32–37.

Clore, G.M. and Schwieters, C.D. (2003) *J. Am. Chem. Soc.*, **125**, 2902–2912.

de la Torre, J.G., Huertas, M.L. and Carrasco, B. (2000) *J. Magn. Reson.*, **147**, 138–146.

Dobrodumov, A. and Gronenborn, A.M. (2003) *Proteins*, **53**, 18–32.

Dominguez, C., Boelens, R. and Bonvin, A.M. (2003) *J. Am. Chem. Soc.*, **125**, 1731–1737.

Dosset, P., Hus, J.C., Blackledge, M. and Marion, D. (2000) *J. Biomol. NMR*, **16**, 23–28.

Fernandez-Recio, J., Totrov, M. and Abagyan, R. (2004) *J. Mol. Biol.*, **335**, 843–865.

Fushman, D., Varadan, R., Assfalg, M. and Walker, O. (2004) *Prog. Nucl. Magn. Reson. Spectrosc.*, **44**, 189–214.

Fushman, D., Xu, R. and Cowburn, D. (1999) *Biochemistry*, **38**, 10225–10230.

Halperin, I., Ma, B., Wolfson, H. and Nussinov, R. (2002) *Proteins*, **47**, 409–443.

Hashimoto, Y., Smith, S.P., Pickford, A.R., Bocquier, A.A., Campbell, I.D. and Werner, J.M. (2000) *J. Biomol. NMR*, **17**, 203–214.

Hus, J.C., Marion, D. and Blackledge, M. (1999) *J. Am. Chem. Soc.*, **121**, 2311–2312.

Hwang, P.M., Skrynnikov, N.R. and Kay, L.E. (2001) *J. Biomol. NMR*, **20**, 83–88.

Schwieters, C.D., Kuszewski, J.J., Tjandra, N. and Clore, G.M. (2003) *J. Magn. Reson.*, **160**, 65–73.

Tjandra, N., Garrett, D.S., Gronenborn, A.M., Bax, A. and Clore, G.M. (1997) *Nat. Struct. Biol.*, **4**, 443–449.

van Dijk, A.D., Fushman, D. and Bonvin, A.M. (2005a) *Proteins*, **60**, 367–381.
van Dijk, A.D.J., Boelens, R. and Bonvin, A.M.J.J. (2005b) *FEBS J.*, **272**, 293–312.
van Nuland, N.A., Hangyi, I.W., van Schaik, R.C., Berendsen, H.J., van Gunsteren, W.F., Scheek, R.M. and Robillard, G.T. (1994) *J. Mol. Biol.*, **237**, 544–559.
Wang, G., Louis, J.M., Sondej, M., Seok, Y.J., Peterkofsky, A. and Clore, G.M. (2000) *EMBO J.*, **19**, 5635–5649.
Worthylake, D., Meadow, N.D., Roseman, S., Liao, D.I., Herzberg, O. and Remington, S.J. (1991) *Proc. Natl. Acad. Sci. USA*, **88**, 10382–10386.